

SPHERICALLY SYMMETRIC SIMULATION WITH BOLTZMANN NEUTRINO TRANSPORT OF CORE COLLAPSE AND POST-BOUNCE EVOLUTION OF A 15 M_⊙ STAR

MARKUS RAMPP¹ AND H.-THOMAS JANKA¹

Draft version October 26, 2018

ABSTRACT

We present a spherically symmetric, Newtonian core-collapse simulation of a 15 M_⊙ star with a 1.28 M_⊙ iron core. The time-, energy-, and angle-dependent transport of electron neutrinos (ν_e) and antineutrinos ($\bar{\nu}_e$) was treated with a new code which iteratively solves the Boltzmann equation and the equations for neutrino number, energy and momentum to order $O(v/c)$ in the velocity v of the stellar medium. The supernova shock expands to a maximum radius of 350 km instead of only ~ 240 km as in a comparable calculation with multi-group flux-limited diffusion (MGFLD) by Bruenn, Mezzacappa, & Dineva (1995). This may be explained by stronger neutrino heating due to the more accurate transport in our model. Nevertheless, after 180 ms of expansion the shock finally recedes to a radius around 250 km (compared to ~ 170 km in the MGFLD run). The effect of an accurate neutrino transport is helpful, but not large enough to cause an explosion of the considered 15 M_⊙ star. Therefore postshock convection and/or an enhancement of the core neutrino luminosity by convection or reduced neutrino opacities in the neutron star seem necessary for neutrino-driven explosions of such stars. We find an electron fraction $Y_e > 0.5$ in the neutrino-heated matter, which suggests that the overproduction problem of neutron-rich nuclei with mass numbers $A \approx 90$ in exploding models may be absent when a Boltzmann solver is used for the ν_e and $\bar{\nu}_e$ transport.

Subject headings: supernovae: general — hydrodynamics — elementary particles — methods: numerical

1. INTRODUCTION

The mechanism of supernova explosions of massive stars is still not satisfactorily understood. Detailed numerical models showed that the hydrodynamic shock, which is launched when the collapsing stellar core bounces abruptly by the stiffening of the equation of state (EoS) at nuclear densities, cannot propagate out promptly but stalls because of energy losses due to photodisintegration of iron-group nuclei and neutrino emission from the shock-heated matter (e.g., Bruenn 1985, 1989a,b; Myra et al. 1987). Early suggestions that energy deposition by neutrinos might cause an explosion reach back to Colgate & White (1966). The modern version of the neutrino-driven “delayed” explosion mechanism is due to Wilson (1985), who found that neutrino energy deposition can revive the stalled shock on a time scale of several hundred milliseconds after bounce (Bethe & Wilson 1985). Because of the complexity of the involved physics and the low efficiency of the neutrino energy transfer it remained unclear for years whether the explosions are sufficiently energetic and whether the delayed mechanism works for a larger range of stellar masses (Wilson et al. 1986; Bruenn 1993). Recognizing that neutron-finger convection in the newly formed neutron star could increase the neutrino luminosities, Wilson & Mayle (1988, 1993) managed to obtain healthy explosions. However, the question of neutron star convection is not finally settled and currently it is not clear whether neutron-finger instabilities or Ledoux convection (Burrows 1987, Pons et al. 1999) or quasi-Ledoux convection (Keil, Janka, & Müller 1996; Janka & Keil 1998) or none (Bruenn et al. 1995; Bruenn & Dineva 1996; Mezzacappa et al. 1998a) occur and how they affect the explosion.

Multi-dimensional hydrodynamic models (Herant et al. 1994; Miller, Wilson, & Mayle 1993; Burrows, Hayes, & Fryxell 1995; Janka & Müller 1996; Mezzacappa et al. 1998b) have demonstrated the existence and the importance of convective overturn in the neutrino-heating layer behind the su-

pernova shock. Driven by a negative entropy gradient which emerges behind the weakening prompt shock and is enhanced by the neutrino energy deposition, the convective motions transport energy from the region of strongest heating to the shock, thus raising the postshock pressure and pushing the shock farther out. At the same time, cold, low-entropy matter is advected downward where it can readily absorb energy from the upstreaming neutrinos. These hydrodynamic instabilities have a bearing on the measured kick velocities of pulsars (Lyne & Lorimer 1994, Cordes & Chernoff 1998) and the anisotropies observed in many supernovae. They are essential to understand the production of radioactive elements in the vicinity of the nascent neutron star and their large-scale mixing into the hydrogen and helium layers of the exploding star (Kifonidis et al. 2000).

All multi-dimensional simulations have so far been carried out with serious simplifications of the neutrino transport. Even the most advanced spherically symmetric post-bounce models have only employed MGFLD (Bruenn 1993, Bruenn et al. 1995) until recently. The significance of an accurate neutrino transport for the delayed explosion mechanism, however, has long been recognized (Janka 1991, Messer et al. 1998, Yamada, Janka, & Suzuki 1999, Burrows et al. 2000). It is therefore a natural step that a new generation of supernova models will employ schemes based on a solution of the Boltzmann equation. In fact, Mezzacappa et al. (2000) have published results for a 13 M_⊙ star which show that a better transport can make a qualitative change to the outcome of the simulations. However, they considered a model with an exceptionally small iron core of 1.17 M_⊙ (Nomoto & Hashimoto 1988) and the explosion energy was only 0.41×10^{51} erg at a post-bounce time of ~ 550 ms. The growth rate of this energy of 0.05×10^{51} erg per 100 ms cannot easily be extrapolated in time and will probably not increase the explosion energy significantly, because the density around the mass cut drops rapidly and the heating region is

¹Max-Planck-Institut für Astrophysik, Karl-Schwarzschild-Str. 1, D-85741 Garching, Germany; mjr@mpa-garching.mpg.de; thj@mpa-garching.mpg.de

evacuated by the developing bifurcation between neutron star and ejecta.

In this *Letter* we present results for a Newtonian simulation of a 15 M_{\odot} star with a 1.28 M_{\odot} iron core (Woosley & Weaver 1995) which show that an accurate neutrino transport does not produce an explosion for this star in spherical symmetry.

2. NUMERICAL METHODS

We have developed a new transport code which determines the neutrino phase-space distribution by iteratively solving the radiation moment equations for neutrino energy and momentum coupled to the Boltzmann equation. The code takes into account effects due to the motion of the stellar medium to order $O(v/c)$ and determines the neutrino quantities in a comoving frame of reference (Rampp 2000; Rampp & Janka 2000, in preparation). It allows a general relativistic treatment, but for comparison with published results we have restricted ourselves to the Newtonian case. The angle dependence of the distribution function is accounted for by the use of a grid of tangent rays which exploits spherical symmetry. Closure of the set of moment equations is achieved by a variable Eddington factor calculated from the solution of the Boltzmann equation, and the integro-differential character of the latter is tamed by making use of the integral moments of the neutrino distribution as obtained from the moment equations. The method is similar to the one described by Burrows et al. (2000). In order to fulfill lepton number conservation, we employ additional moment equations for neutrino number density and number flux. Severe time step restrictions are avoided and proper establishment of equilibrium is ensured by integrating the set of transport equations implicitly in time. The stiff character of the source terms for neutrino energy and lepton number requires a simultaneous implicit update of the temperature and electron fraction of the stellar medium.

The transport is coupled to the hydrodynamics code *Prometheus*, which integrates the continuity equations for mass, momentum, energy and particle species in a conservative way on a moving radial grid by explicit time stepping. The integration is accurate to second order in space and time. Shocks are treated as local Riemann problems at the zone interfaces (Fryxell, Müller & Arnett 1989). The source terms for energy and momentum due to gravity and neutrinos, and for lepton number due to neutrino emission/absorption are handled by an operator-splitting technique. The stellar background and the neutrinos are evolved on different radial grids and with different time steps, which are constrained by changes per transport step (which is typically larger than the hydrodynamical step) of at most 10% for the neutrino quantities and 5% for the fluid quantities. Interpolation between both grids is done in a conservative manner.

We used the EoS of Lattimer & Swesty (1991) (with nuclear incompressibility modulus of $K = 180$ MeV) which is extended to densities and temperatures below the regime of nuclear statistical equilibrium by an ideal gas equation of state, corrected for Coulomb-lattice effects, that includes arbitrarily relativistic and degenerate electrons and positrons, photons, and a mixture of predefined nuclear species. Nuclear burning was not taken into account in the present simulation.

The hydrodynamics was solved on a grid with 400 radial zones out to 20000 km, which were moved with the matter of the iron core during collapse to ensure good spatial resolution at all times, and kept fixed later. For the transport we used a Eulerian grid with 210 geometrically spaced radial zones, 230

tangent rays and 27 energy bins geometrically distributed between 0 and 380 MeV, the zone center of the first zone being at 1 MeV. The quality of the energy conservation limits the error in the net energy deposition by neutrinos to $< 5 \times 10^{49}$ erg, and lepton number is globally conserved to better than 0.1%.

The present simulation includes only ν_e and $\bar{\nu}_e$. The corresponding rates for charged-current and neutral-current reactions with nucleons and nuclei and for neutrino-electron scattering were taken from Bruenn (1985), Mezzacappa & Bruenn (1993) and Bruenn & Mezzacappa (1997). We neglect production and annihilation of $\nu_e\bar{\nu}_e$ pairs, which are of minor importance compared to the charged-current reactions with nucleons. A detailed comparison of core-collapse results with published models of Bruenn & Mezzacappa (1997) showed excellent agreement. Disregarding muon and tau neutrinos and antineutrinos and $\nu_e\bar{\nu}_e$ pair processes has virtually no effect on the neutrino heating (see Bruenn 1993).

3. RESULTS

Figure 1 shows the trajectories of selected mass shells as a function of time. The bounce shock forms 211.6 ms after the onset of the collapse at a radius of 12.5 km with an enclosed mass of $\sim 0.62 M_{\odot}$. The central density at this time is $\rho_c = 3.3 \times 10^{14} \text{ g cm}^{-3}$ (cf. Bruenn & Mezzacappa 1997). By the rapid accretion of mass (Fig. 2) the shock is pushed out to ~ 240 km. When the accretion rate drops significantly at ~ 120 ms after bounce, neutrino heating is able to support further shock expansion to a radius of 350 km. After some time, however, the shock retreats again and finally turns into a standing accretion shock around 250 km, still within the collapsing silicon shell of the progenitor star. No indication for the possibility of an explosion was visible when the simulation was terminated at 350 ms after bounce. At this time the shock was stagnant and enclosed a mass of 1.5 M_{\odot} with increasingly negative postshock velocities. The decreasing density in the neutrino-heating region and the decay of the ν_e and $\bar{\nu}_e$ luminosities do not give hope for a later rejuvenation of the shock. The overall evolution in our simulation is very similar to model WPE15ls(180)Newt20 in Bruenn et al. (1995), who used MGFLD for the neutrino transport. The most obvious difference is a larger maximum radius of the shock, 350 km compared to only ~ 240 km in the calculation by Bruenn et al. (1995). Also, the shock is able to stay near its maximum radius for a longer time and afterwards does not recede as far as in model WPE15ls(180)Newt20.

The ν_e and $\bar{\nu}_e$ luminosities and the root-mean-squared energies at 1000 km are shown as functions of time in Fig. 2. The prompt ν_e burst with a peak luminosity of $3.36 \times 10^{53} \text{ erg s}^{-1}$ arrives at this radius only ~ 6 ms after core bounce. About 50 ms after bounce the ν_e and $\bar{\nu}_e$ luminosities have become roughly equal with a fairly stable value of $(2.5-3) \times 10^{52} \text{ erg s}^{-1}$. By the end of our simulation they begin to decrease slowly, different from the mean energies, which show a gradual rise to 11.2 MeV for ν_e and 15.5 MeV for $\bar{\nu}_e$.

In Fig. 3 we present profiles of the net energy deposition rate by ν_e and $\bar{\nu}_e$, of the electron fraction Y_e and of the entropy per baryon for times 330 ms, 380 ms and 561 ms. The gain radius, below which net neutrino cooling and above which net heating occurs, is at 120–140 km (see also Fig. 1). The heating rates peak somewhat outside the gain radius and reach up to $\sim 120 \text{ MeV s}^{-1}$ per baryon. The cooling rate below the gain radius can exceed 200 MeV s^{-1} per baryon at late times. Maximum entropies around 13 k_B per nucleon are seen at the end of the sim-

ulation, when the density behind the shock is lowest because of the decreasing mass accretion rate. The negative entropy gradient implies potential instability against convective overturn in the region between maximum heating and supernova shock. In this layer Y_e climbs to values *larger* than 0.5 and also develops a negative gradient. Values $Y_e > 0.5$ were also found by Mezzacappa et al. (2000) in the neutrino-heated ejecta behind the outgoing shock for the successful explosion of a $13 M_\odot$ star. The neutronization of the neutrino-heated medium is determined by the absorption of ν_e on neutrons and of $\bar{\nu}_e$ on protons and the inverse processes. It is sensitive to the luminosities and spectra but also to the angular distributions of the neutrinos in the heating region, which govern the efficiency of energy deposition as well as the lepton exchange with the medium. Since ν_e decouple at a larger radius than $\bar{\nu}_e$, their distribution is more isotropic in the heating region, leading to a higher probability of ν_e absorption and thus to an increase of Y_e . This is enhanced by the recombination of α particles (Fuller & Meyer 1995).

4. CONCLUSIONS

Our spherically symmetric, Newtonian simulation of a $15 M_\odot$ star with a $1.28 M_\odot$ iron core, using a new Boltzmann solver for the neutrino transport, did not give an explosion until 350 ms after core bounce, although the shock reached a larger maximum radius than in a comparable MGFLD simulation of Bruenn et al. (1995). This is probably explained by stronger neutrino heating of the postshock medium with the more accurate Boltzmann transport. Since both simulations were done with the same progenitor, EoS, and neutrino opacities, and excellent agreement during the core-collapse phase was found, uncertainties due to the different numerics seem to be minimized. Although we have only included ν_e and $\bar{\nu}_e$ in our simulation, we consider our conclusions as solid, because muon and tau neutrinos would drain energy from the ν_e and $\bar{\nu}_e$ luminosities but contribute to the postshock heating only at an insignificant level due to the lack of charged-current interactions. The main effect of adding pair processes would be a weakening of

the early shock propagation by additional energy losses. Also general relativity would probably hamper an explosion (Fryer 1999), but the situation is still ambiguous (De Nisco, Bruenn, & Mezzacappa 1998; Baron 1988).

The importance of an accurate ν_e and $\bar{\nu}_e$ transport is emphasized by the finding that $Y_e > 0.5$ in the region of net neutrino energy deposition. This is interesting because $Y_e \lesssim 0.48$ was obtained in the neutrino-heated ejecta in supernova models, e.g., by Herant et al. (1994), Burrows et al. (1995) and Janka & Müller (1996), causing a large overproduction of neutron-rich nuclei around $N = 50$ and $A \approx 90$ (^{88}Sr , ^{89}Y , ^{90}Zr). This is in conflict with measured galactic abundances. With values $Y_e > 0.5$ this problem disappears (Hoffman et al. 1996).

Using their Boltzmann solver for the neutrino transport, Mezzacappa et al. (2000) obtained a successful, but weak explosion in case of a $13 M_\odot$ progenitor with an extraordinarily small iron core of $1.17 M_\odot$. For a $15 M_\odot$ star with a larger core (and therefore most likely also for more massive progenitors), we cannot confirm a qualitative difference from spherically symmetric simulations with MGFLD transport, although we find important quantitative differences with our more accurate neutrino transport. In order to obtain explosions via the neutrino-heating mechanism, multi-dimensional simulations seem indispensable for stars with typical iron core masses. Convection inside the neutron star (Keil et al. 1996) or lower neutrino opacities — due to suppression relative to the standard description by nucleon correlation effects (e.g., Janka et al. 1996, Burrows & Sawyer 1998, Reddy et al. 1999) — could raise the neutrino emission significantly on the relevant time scale of a few 100 ms after bounce, and convective overturn in the postshock region has been shown by several groups to support the explosion.

Support by Deutsche Forschungsgemeinschaft grant SFB 375 für Astro-Teilchenphysik is acknowledged. The NEC SX-5/3C of the Rechenzentrum Garching was used for the computations.

REFERENCES

- Baron, E. 1988, *Phys. Rep.*, 163, 37
 Bethe, H.A., & Wilson, J.R. 1985, *ApJ*, 295, 14
 Bruenn, S.W. 1985, *ApJ Suppl.*, 58, 771
 Bruenn, S.W. 1989a, *ApJ*, 340, 955
 Bruenn, S.W. 1989b, *ApJ*, 341, 385
 Bruenn, S.W. 1993, in *Nuclear Physics in the Universe*, eds. Guidry M.W. and Strayer M.R., IOP, Bristol, p. 31
 Bruenn, S.W., & Dineva, T. 1996, *ApJ*, 458, L71
 Bruenn, S.W., & Mezzacappa, A. 1997, *Phys. Rev. D*, 56, 7529
 Bruenn, S.W., Mezzacappa, A., & Dineva, T. 1995, *Phys. Rep.*, 256, 69
 Burrows, A. 1987, *ApJ*, 318, L57
 Burrows, A., & Sawyer, R.F. 1998, *Phys. Rev. C*, 58, 554
 Burrows, A., Hayes, J., & Fryxell, B.A. 1995, *ApJ*, 450, 830
 Burrows, A., Young, T., Pinto, P.A., Eastman, R., & Thompson, T. 2000, *ApJ*, in press (astro-ph/9905132)
 Colgate, S.A., & White, R.H. 1966, *ApJ*, 143, 626
 Cordes, J.M., & Chernoff, D.F. 1998, *ApJ*, 505, 315
 De Nisco, K.R., Bruenn, S.W., & Mezzacappa, A. 1998, in *Stellar Evolution, Stellar Explosions and Galactic Chemical Evolution*, ed. Mezzacappa A., IOP, Bristol, p. 571
 Fryer, C.L. 1999, *ApJ*, 522, 413
 Fryxell, B.A., Müller, E., & Arnett, W.D. 1989, MPA-Preprint 449, Garching
 Fuller, G.M., & Meyer, B.S. 1995, *ApJ*, 453, 792
 Herant, M., Benz, W., Hix, W.R., Fryer, C.L., & Colgate, S.A. 1994, *ApJ*, 435, 339
 Hoffman, R.D., Woosley, S.E., Fuller, G.M., & Meyer, B.S. 1996, *ApJ*, 460, 478
 Janka, H.-Th. 1991, PhD Thesis, TU München, MPA-Report 587
 Janka, H.-Th., & Keil, W. 1998, in *Supernovae & Cosmology*, eds. Labhardt L., Binggeli B., and Buser R., Astron. Inst. Univ. Basel, p. 7 (astro-ph/9709012)
 Janka, H.-Th., & Müller, E. 1996, *A&A*, 306, 167
 Janka, H.-Th., Keil, W., Raffelt, G., & Seckel, D. 1996, *Phys. Rev. Lett.*, 76, 2621
 Keil, W., Janka, H.-Th., & Müller, E. 1996, *ApJ*, 473, L111
 Kifonidis, K., Plewa, T., Janka, H.-Th., & Müller, E. 2000, *ApJ*, 531, L123
 Lattimer, J.M., & Swesty, F.D. 1991, *Nucl. Phys.*, A535, 331
 Lyne, A., & Lorimer, D.R. 1994, *Nature*, 369, 127
 Mayle, R., & Wilson, J.R. 1988, *ApJ*, 334, 909
 Messer, O.E.B., Mezzacappa, A., Bruenn, S.W., & Guidry, M.W., 1998, *ApJ*, 507, 353
 Mezzacappa, A., & Bruenn, S.W. 1993, *ApJ*, 405, 637
 Mezzacappa, A., Calder, A.C., Bruenn, S.W., Blondin, J.M., Guidry, M.W., Strayer, M.R., & Umar, A.S. 1998a, *ApJ*, 493, 848
 Mezzacappa, A., Calder, A.C., Bruenn, S.W., Blondin, J.M., Guidry, M.W., Strayer, M.R., & Umar, A.S. 1998b, *ApJ*, 495, 911
 Mezzacappa, A., Liebendörfer, M., Messer, O.E.B., Hix, W.R., Thielemann, F.-K., & Bruenn, S.W. 2000, *Phys. Rev. Lett.*, subm. (astro-ph/0005366)
 Müller, D.S., Wilson, J.R., & Mayle, R.W. 1993, *ApJ*, 415, 278
 Myra, E.S., Bludman, S.A., Hoffman, Y., Lichtenstadt, I., Sack, N., & Van Riper, K.A. 1987, *ApJ*, 318, 744
 Nomoto, K., & Hashimoto, M. 1988, *Phys. Rep.*, 163, 13
 Pons, J.A., Reddy, S., Prakash, M., Lattimer, J.M., & Miralles, J.A. 1999, *ApJ*, 513, 780
 Rampp, M. 2000, PhD Thesis, TU München
 Reddy, S., Prakash, M., Lattimer, J.M., & Pons, J.A. 1999, *Phys. Rev. C*, 59, 2888
 Wilson, J.R. 1985, in *Numerical Astrophysics*, eds. J.M. Centrella, J.M. LeBlanc, R.L. Bowers, Jones and Bartlett, Boston, p. 422
 Wilson, J.R., & Mayle R. 1988, *Phys. Rep.*, 163, 63
 Wilson, J.R., & Mayle R. 1993, *Phys. Rep.*, 227, 97
 Wilson, J.R., Mayle, R., Woosley, S.E., & Weaver, T. 1986, *Ann. NY Acad. Sci.*, 470, 267

Woosley, S.E., & Weaver, T.A. 1995, ApJ Suppl., 101, 181

Yamada, S., Janka, H.-Th., & Suzuki, H. 1999, A&A, 344, 533

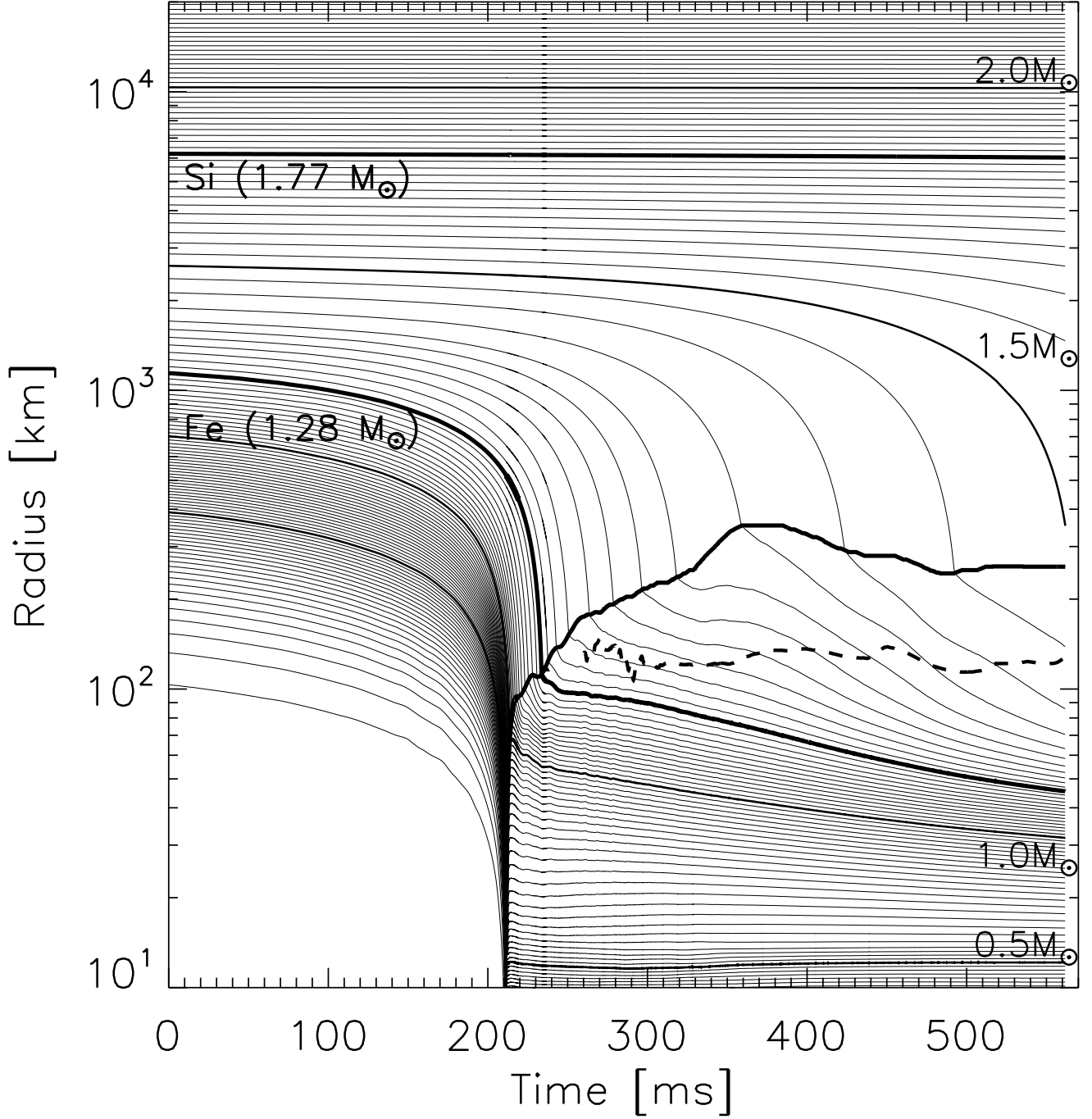


FIG. 1. — Trajectories of selected mass shells vs. time from the start of the simulation. The shells are equidistantly spaced in steps of $0.02 M_{\odot}$, and the trajectories of the outer boundaries of the iron core (at $1.28 M_{\odot}$) and of the silicon shell (at $1.77 M_{\odot}$) are indicated by bold lines. The shock is formed at 211 ms. Its position is also marked by a bold line. The dashed curve shows the position of the gain radius.

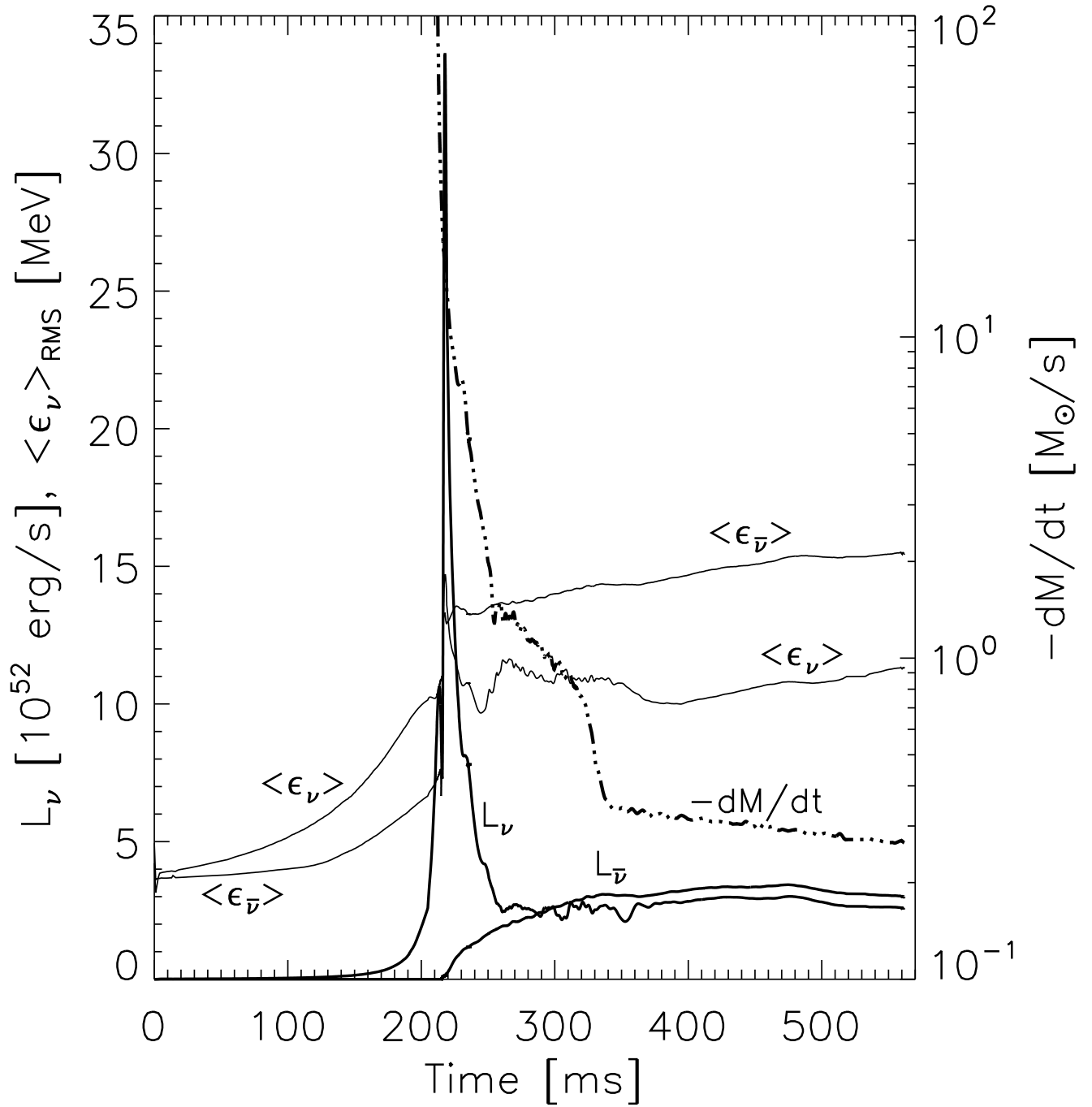


FIG. 2.— Comoving frame electron neutrino and antineutrino luminosities (bold solid lines) and rms energies (thin solid lines) at 1000km as functions of time. Also shown is the mass accretion rate through the shock (dashed-dotted line, scale on the right ordinate).

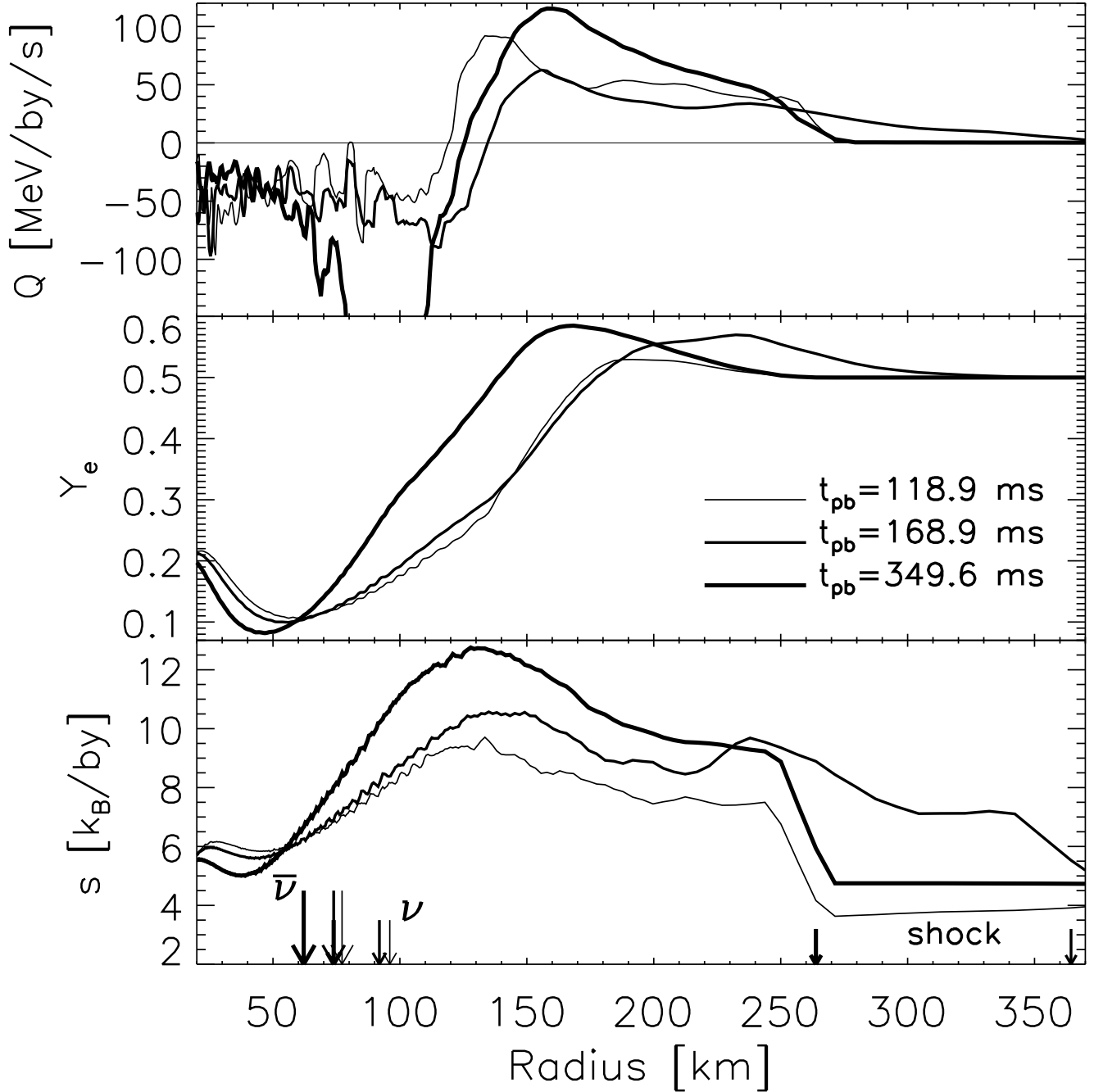


FIG. 3.— Radial profiles of the net energy deposition rate by ν_e and $\bar{\nu}_e$, Q , (top), of the electron fraction Y_e (middle) and of the entropy per baryon, s , (bottom) at times 119 ms (thin lines), 169 ms (medium lines) and 350 ms (bold lines) after core bounce. The positions of the shock and of the ν_e - and $\bar{\nu}_e$ -spheres are indicated.